ISSN 1674-1056
http://cpb.iphy.ac.cn
http://iopscience.iop.org/cpb
中国物理 B
Chinese Physics
中国物理 Chinese Physics B

Domain walls and their interactions in a two-component Bose-Einstein condensate

Ling-Zheng Meng(孟令正), Yan-Hong Qin(秦艳红), Li-Chen Zhao(赵立臣), Zhan-Ying Yang(杨战营)
Citation: Chin. Phys. B . 2019, 28(6): 060502. **doi:** 10.1088/1674-1056/28/6/060502
Journal homepage: http://cpb.iphy.ac.cn; http://iopscience.iop.org/cpb

What follows is a list of articles you may be interested in

Domain walls and their interactions in a two-component Bose-Einstein condensate

Ling-Zheng Meng(孟令正), Yan-Hong Qin(秦艳红), Li-Chen Zhao(赵立臣), Zhan-Ying Yang(杨战营)
Chin. Phys. B . 2019, 28(6): 060502. **doi:** 10.1088/1674-1056/28/6/060502

Formation mechanism of asymmetric breather and rogue waves in pair-transition-coupled nonlinear Schrödinger equations

Zai-Dong Li(李再东), Yang-yang Wang(王洋洋), Peng-Bin He(贺鹏斌)
Chin. Phys. B . 2019, 28(1): 010504. **doi:** 10.1088/1674-1056/28/1/010504

Solitons in nonlinear systems and eigen-states in quantum wells

Li-Chen Zhao(赵立臣), Zhan-Ying Yang(杨战营), Wen-Li Yang(杨文力)
Chin. Phys. B . 2019, 28(1): 010501. **doi:** 10.1088/1674-1056/28/1/010501

Symmetry and asymmetry rogue waves in two-component coupled nonlinear Schrödinger equations

Zai-Dong Li(李再东), Cong-Zhe Huo(霍丛哲), Qiu-Yan Li(李秋艳), Peng-Bin He(贺鹏斌), Tian-Fu Xu(徐天赋)
Chin. Phys. B . 2018, 27(4): 040505. **doi:** 10.1088/1674-1056/27/4/040505

Soliton structures in the (1+1)-dimensional Ginzburg-Landau equation with a parity-time-symmetric potential in ultrafast optics

Wenyi Li(李文义), Guoli Ma(马国利), Weitian Yu(于维天), Yujia Zhang(张玉佳), Mengli Liu(刘孟丽), Chunyu Yang(杨春玉), Wenjun Liu(刘文军)
Chin. Phys. B . 2018, 27(3): 030504. **doi:** 10.1088/1674-1056/27/3/030504

Domain walls and their interactions in a two-component Bose–Einstein condensate*

Ling-Zheng Meng(孟令正), Yan-Hong Qin(秦艳红), Li-Chen Zhao(赵立臣)†, and Zhan-Ying Yang(杨战营)

Shaanxi Key Laboratory for Theoretical Physics Frontiers, School of Physics, Northwest University, Xi'an 710069, *China*

(Received 30 January 2019; revised manuscript received 13 March 2019; published online 29 May 2019)

We investigate domain wall excitations in a two-component Bose–Einstein condensate with two-body interactions and pair-transition effects. It is shown that domain wall excitations can be described exactly by kink and anti-kink excitations in each component. The domain wall solutions are given analytically, which exist with different conditions compared with the domain wall reported before. Bubble-droplet structure can be also obtained from the fundamental domain wall, and their interactions are investigated analytically. Especially, domain wall interactions demonstrate some striking particle transition dynamics. These striking transition effects make the domain wall admit quite different collision behavior, in contrast to the collision between solitons or other nonlinear waves. The collisions between kinks induce some phase shift, which makes the domain wall change greatly. Their collisions can be elastic or inelastic with proper combination of fundamental domain walls. These characters can be used to manipulate one domain wall by interacting with other ones.

Keywords: domain wall, pair-transition, multi-component Bose–Einstein condensate

PACS: 05.45.Yv, 02.30.Ik, 42.65.Tg **DOI:** 10.1088/1674-1056/28/6/060502

1. Introduction

Multi-component coupled Bose–Einstein condensate (BEC) provides a good platform to study dynamics of vector solitons.[1,2] Many different vector solitons have been obtained in two-component coupled BEC systems, such as bright–bright soliton,[3] bright–dark soliton,[4] dark–bright soliton,[5–7] dark–dark soliton.[8] Moreover, it is possible to find dark–anti-dark soliton in BEC with unequal inter- and intra-species interaction strengths.[9–12] If the superposition of the dark soliton and anti-dark soliton in two components is uniform density, the dark–anti-dark soliton would become the so-called "magnetic soliton".[9,10] Different from the magnetic properties of these solitons, domain wall (DW) can also exist in two-component BEC with many different settings.[13–16] Furthermore, exact analytical domain wall solutions were derived with both two-body and three-body interactions in a two-component BEC system.[17] The DW solutions usually correspond to kink and anti-kink excitations in each component. With linear coupling effects, an exact DW solution was produced for ratio 3:1 of the inter-species and intra-species interaction coefficients.[18] But the interactions between DWs or their motions were investigated numerically in the most of previously studies. Based on the most of previous studies on vector solitons in two-component BEC, we can know that kink-type excitation can not be obtained with identical inter-species and intra-species interaction strengths.[19–21] Therefore we try to find kink and anti-kink excitations in some integrable cases with different inter-species and intra-species interaction strengths. The integrability could enable us to discuss the interactions between DWs more clearly and conveniently.

We note that pair-transition effects bring many striking localized wave structures in a two-component BEC,[22–26] since the constrain conditions on nonlinear interactions are quite different from the ones in Manakov model.[27] For this integrable case with the pair-transition effects, the inter-species and intra-species interaction strengths can be different. This provides possibilities to investigate nonlinear waves exactly and analytically in the system. Moreover, experiments in BEC systems suggested that pair-particle transition effect became dominant, and single-particle transition could be ignored.[28,29] We therefore try to look for kink and anti-kink excitations in the system. Moreover, more exotic transition dynamics are expected to exist in the pair-transition coupled model,[24,26] compared with transition process for DWs obtained in Refs. [17] and [18].

In this paper, we show that DW excitation can exist in a two-component BEC with pair-transition effects. It is shown that DW excitations can be described exactly by kink and anti-kink excitations in each component. The DW with moving velocities can be described by a generic solution. The DW solutions are given analytically with no three-body interactions, in contrast to the DW reported before.[17] The explicit conditions are for ratio 2:1 of the inter-species and intra-species interaction coefficients, which is different from the ones obtained in BEC with linear inter-conversion between the immiscible

*Project supported by the National Natural Science Foundation of China (Grant No. 11775176), the Major Basic Research Program of the Natural Science Foundation of Shaanxi Province, China (Grant No. 2018KJXX-094), and the Key Innovative Research Team of Quantum Many-Body Theory and Quantum Control in Shaanxi Province, China (Grant No. 2017KCT-12).

†Corresponding author. E-mail: zhaolichen3@nwu.edu.cn

© 2019 Chinese Physical Society and IOP Publishing Ltd

components.[18] Furthermore, we derive multi-kink in the system, which can be used to investigate nonlinear interactions between DWs exactly. And in this way, bubble-droplet structure can be obtained. Especially, their interactions demonstrate some striking particle transition dynamics. The striking transition effects make the DW admit quite different collision behavior, in contrast to the collision between solitons or other nonlinear waves. The collisions between kinks induce phase shift, which makes the DW change greatly. With the proper combination of fundamental DWs, collisions can be elastic or inelastic. These characters can be used to manipulate one DW by interacting with other ones.

2. Physical model

One-dimensional two-component BEC system with particle transition can be described by the Hamiltonian

$$\hat{H}=\sum_i\left[-\frac{\hbar^2}{2m}\partial_x^2\hat{q}_i\hat{q}_i^\dagger+\frac{g_{i,i}}{2}\hat{n}_i\hat{n}_i+g_{i,3-i}\hat{n}_i\hat{n}_{3-i}+J_1(\hat{q}_j^\dagger\hat{q}_{3-j}+\hat{q}_{3-j}^\dagger\hat{q}_j)+\frac{J_2}{2}(\hat{q}_i^\dagger\hat{q}_i^\dagger\hat{q}_{3-i}\hat{q}_{3-i}+\hat{q}_{3-i}^\dagger\hat{q}_{3-i}^\dagger\hat{q}_i\hat{q}_i)\right],$$

where $n_i=\hat{q}_i^\dagger\hat{q}_i$ is the particle number operator, the symbol † represents the Hermite conjugation. $g_{i,i}$ and $g_{3-i,i}$ $(i=1,2)$ are the intra- and inter-species interactions between atoms. J_1 and J_2 denote single particle transition and pair particle transition coupling strengths,[30,31] the pair particle transition terms correspond to pair-transition effects in BEC or the four-wave-mixing in optic systems. Recent experimental results in a double-well Bose–Einstein condensate suggested that pair-transition can become dominant with strong interaction between atoms.[28,29] Therefore, we consider that the case for second-order transition is dominant, namely, $J_1=0$ and $J_2\neq 0$. The corresponding dynamic evolution equation can be derived from the Heisenberg equation $\mathrm{i}\hbar(\partial\hat{q}_i/\partial t)=[\hat{q}_i,\hat{H}]$ for the field operator. Performing the mean field approximation $\langle\hat{q}_j\rangle=q_j$, we can get the following integrable coupled nonlinear Schrödinger equations (NLSE) in dimensionless form $m=\hbar=1$,

$$\begin{aligned}&\mathrm{i}q_{1,t}+\frac{1}{2}q_{1,xx}-(|q_1|^2+2|q_2|^2)q_1-q_2^2\bar{q}_1=0,\\&\mathrm{i}q_{2,t}+\frac{1}{2}q_{2,xx}-(2|q_1|^2+|q_2|^2)q_2-q_1^2\bar{q}_2=0,\end{aligned}\tag{1}$$

where q_1 and q_2 are functions of the space coordinate x and time t, the symbol overbar represents the complex conjugation. Many striking localized wave structures had been given in two-component BEC,[22–26] as the constrain conditions on nonlinear interactions are quite different from the ones in Manakov model. Since the dark soliton admits kink-like character partly, we will start from investigating dark soliton combing with some other nonlinear waves. Notably, a linear superposition of dark soliton with a nonlinear plane wave can produce kink-like density distribution. This is a key clue to construct DW in BEC with pair-transition effects. With the aid of linear superposition of dark soliton solutions and a general plane wave, we obtain DWs exactly and analytically, this is the main result of this paper. Next, we show the DWs explicitly and investigate the transition behavior during their interaction processes.

3. Analytical domain wall and bubble-droplet solution

3.1. Domain wall solution

The fundamental DW solution can be derived as follows, it is similar to the solutions reported in Refs. [25] and [32]:

$$\begin{aligned}q_1=&\frac{1}{2}\{[1-F_1+F_1\tanh(G_1)]c_1\,\mathrm{e}^{\mathrm{i}(k_1x-\omega_1t)}\\&+c_2\,\mathrm{e}^{\mathrm{i}(k_2x-\omega_2t)}\},\end{aligned}\tag{2}$$

$$\begin{aligned}q_2=&\frac{1}{2}\{[1-F_1+F_1\tanh(G_1)]c_1e^{\mathrm{i}(k_1x-\omega_1t)}\\&-c_2\,\mathrm{e}^{\mathrm{i}(k_2x-\omega_2t)}\},\end{aligned}\tag{3}$$

where

$$\begin{aligned}&F_j=\mathrm{i}\mu_{\mathrm{I},j}/(\lambda_j-\mu_{\mathrm{R},j}+\mathrm{i}\mu_{\mathrm{I},j}),\\&G_j=\mu_{\mathrm{I},j}[x+(\lambda_j+\mu_{\mathrm{R},j})t+\alpha_j],\\&\mu_{\mathrm{R},j}=-k_i/2,\\&\mu_{\mathrm{I},j}=-\sqrt{4c_i^2-(k_i+2\lambda_j)^2}/2,\\&\omega_i=(2c_i^2+k_i^2)/2.\end{aligned}$$

The real parameter λ_j $(j=1,2)$ is the spectral parameter, $\mu_{\mathrm{R},j}$ and $\mu_{\mathrm{I},j}$ are the real and imaginary part of μ_j which is root of the characteristic equation. c_i, k_i, and ω_i are the background amplitudes, wave vectors, and frequencies of the dark soliton and plane wave, α_j only affect the center position of DW. The parameters c_i, k_i, and λ_j satisfy the following formula $4c_i^2-(k_i+2\lambda_j)^2>0$, otherwise the solution will not exist.

Based on the solution, we can observe the profiles of DW conveniently. As an example, we show the simplest case for fundamental DW. With $c_1=c_2$, $k_1=k_2$, stable domain wall structure can be shown in Fig. 1, the stability of DW is tested numerically with some weak noises, the results indicate that the DW is stable. This DW solution is different from the exact solutions in Refs. [17] and [18] that it is not completely static. The moving DW was investigated numerically by adding a spatial-dependent phase.[17,18] Moreover, many different profiles appear when the spectral parameter or background parameters vary, we can control the velocity, height and gradient of

DW by adjusting the value of λ_j, this gives us the opportunity to study the interaction of DWs analytically. When c_j or k_j is changed and results in $k_1 - k_2 \neq 0$ or $\omega_1 - \omega_2 \neq 0$, the stable DW and anti-DW will disappear as the backgrounds oscillate periodically. We do not show these cases, since their properties are similar to the one in Fig. 1, just with some additional spatial-temporal periodic behaviors.

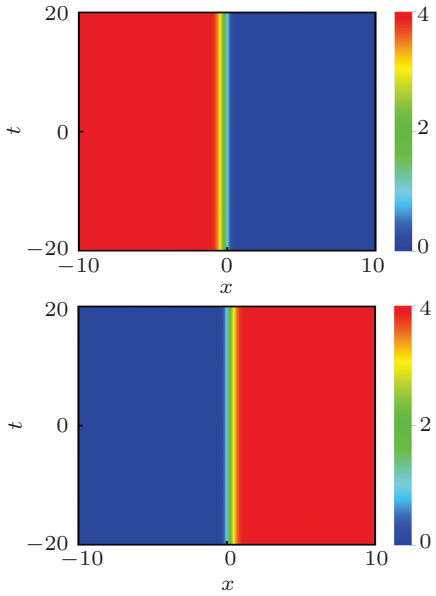


Fig. 1. The density distribution of two components for fundamental domain wall. The upper one is a kink in q_1 component, and the lower one is an anti-kink in q_2 component. This is a static domain wall, its stability is tested numerically against weak noises. The moving domain wall can be also demonstrated by the exact solution. The parameters are $\lambda_1 = 0.01$, $k_1 = k_2 = 0.02$, $c_1 = c_2 = 2$, and $\alpha = 0$.

3.2. Bubble-droplet states

A striking bubble-droplet structure can be obtained through combining a DW and an anti-DW properly. If the domain wall and the anti-domain wall admit identical velocities, the solution for bubble-droplet structure can be written as:

$$\begin{aligned} q_1 = \frac{1}{2}\{&[1 - F_1 + F_1 \tanh(G_1)]c_1 \mathrm{e}^{\mathrm{i}(k_1 x - \omega_1 t)} \\ &+ [1 - F_2 + F_2 \tanh(G_2)]c_2 \mathrm{e}^{\mathrm{i}(k_2 x - \omega_2 t)}\}, \\ q_2 = \frac{1}{2}\{&[1 - F_1 + F_1 \tanh(G_1)]c_1 \mathrm{e}^{\mathrm{i}(k_1 x - \omega_1 t)} \\ &- [1 - F_2 + F_2 \tanh(G_2)]c_2 \mathrm{e}^{\mathrm{i}(k_2 x - \omega_2 t)}\}. \end{aligned} \tag{4}$$

The implications of parameters are the same as in Subsection 3.1. If only α_1 and α_2 are of unequal values and other parameters are equal respectively, the profile of this solution corresponds to bubble-droplet. The numerical results of this structure and its evolution with no velocity in BEC have been reported before,[17,18] now we give an exact analytical solution, and bubble-droplet state can be non-static, its velocity can be adjusted by changing the values of λ_j too. As an example, we show one static case in Fig. 2. It is seen that kink–anti-kink structure appears in the two components and they are parallel. The profiles could be considered as a bubble coupled to a droplet, which refers to as bubble-droplet state. When the distance between DWs and anti-DWs are small enough, the cross section of two components can be approximately regarded as a dark soliton and a bright soliton. The dark–bright soliton is similar to dark–bright one obtained in two-component BEC system, but the expressions of them are distinctive, which makes them possess different effective mass.The stability of bubble-droplet state is tested numerically with weak white noises, and its long time evolution is shown in Fig. 3. The results of simulation indicate that bubble-droplet we construct can be stable with weak noises.

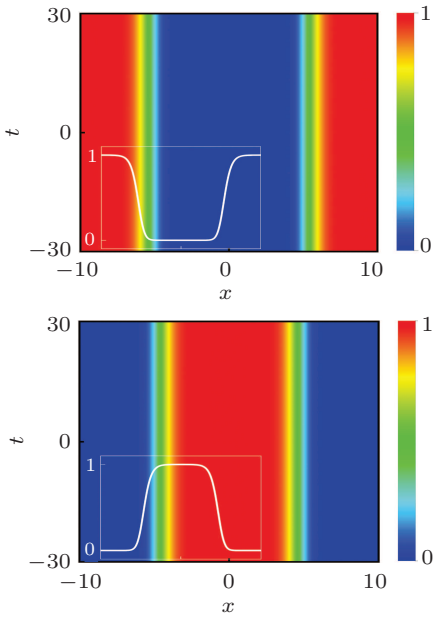


Fig. 2. Density map and profiles of bubble-droplet state, the upper one is the bubble (sort of dark soliton) component, the lower one is droplet (bright soliton) component. It is seen that the structures are constituted of a domain wall combined with a paralleled anti-domain wall. The parameters are $\lambda_1 = \lambda_2 = 0.01$, $k_1 = k_2 = 0.02$, $c_1 = c_2 = 1$, $-\alpha_1 = \alpha_2 = 4$.

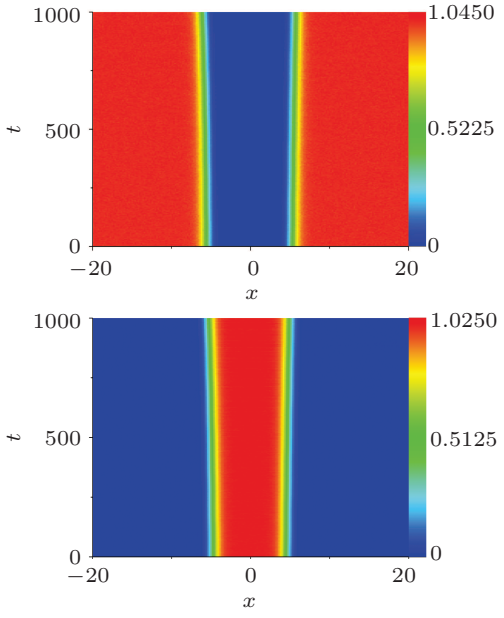


Fig. 3. Density map of the evolution of bubble-droplet with weak random noises, it is clear that this state can be robust against weak noises. The parameters are $\lambda_1 = \lambda_2 = 0.01$, $k_1 = k_2 = 0.02$, $c_1 = c_2 = 1$, $-\alpha_1 = \alpha_2 = 4$.

If $\lambda_1 \neq \lambda_2$, the kink and anti-kink will have different velocities. The solution can be used to investigate the interactions between DWs. We note that the interaction processes admit abundant transition behavior between the two components. We can investigate the interactions between DWs and bubble-droplets conveniently through deriving high-order DW solutions.

4. Particles transition during the interaction process between domain walls

When the velocities of DW and anti-DW are different, they will collide somewhere and induce new dynamical behavior. From Fig. 4, we can see that parallel and non-parallel situations have completely different properties. In the non-parallel case, stable bubble-droplet state disappears and the backgrounds become asymmetric both in two components. Neither interference behavior nor the tunneling of particles emerges during the collision process, which is different from our previous work on wave properties of solitons.[33,34] However, the parts between kink and anti-kink have different values before and after the collision, this means that the particles are no longer conserved in each component. The particle transition emerges between two components, with the total number of particles in the whole system is constant.

In order to investigate the transition behavior, we numerically calculate the changes in the number of particles of the two components while domain walls interact with each other in Fig. 4. The particle number evolutions for the two components are shown in Fig. 5, which is calculated in the regimes where particle transition happens. It is obvious that there is a transition behavior between the two components, the particles transit in pairs and the total number of them in the whole system is constant. The phase shift induced by the collision can be used to explain why the particle numbers vary.[26]

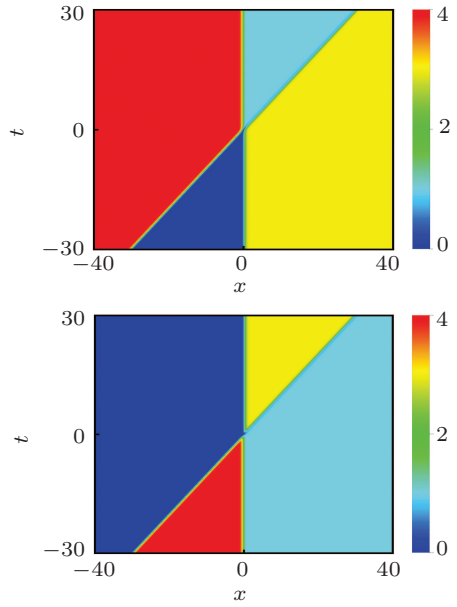


Fig. 4. Density map of collision between domain wall and anti-domain wall. It is seen that the profiles of parts between kink and anti-kink in each component both vary greatly after the collision, the kinks' profiles flipped over. The parameters are $\lambda_1 = -0.5$, $\lambda_2 = 0.5$, $k_1 = k_2 = 1$, $c_1 = c_2 = 2$, $\alpha_1 = \alpha_2 = 0$.

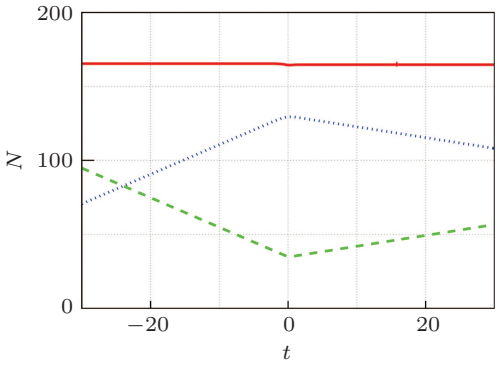


Fig. 5. Particle number's evolutions of the two components in regime of $[-35, 35]$, where the particle transition happens. The blue dotted line represents bubble component, the green dashed line represents droplet component, and the thick red line represents total number of particles in this regime. The parameters are $\lambda_1 = -0.5$, $\lambda_2 = 0.5$, $k_1 = k_2 = 1$, $c_1 = c_2 = 2$, $\alpha_1 = \alpha_2 = 0$.

Then, we further investigate the collision between a DW and a bubble-droplet. Solution for describing the interaction between DW and bubble-droplet can be derived as

$$
\begin{aligned}
q_1 &= \frac{1}{2}\{c_1 \frac{|M_i|}{|M|} e^{i(k_1 x - \omega_1 t)} + [1 - F_3 + F_3 \tanh(G_3)] c_2 e^{i(k_2 x - \omega_2 t)}\}, \\
q_2 &= \frac{1}{2}\{c_1 \frac{|M_i|}{|M|} e^{i(k_1 x - \omega_1 t)} - [1 - F_3 + F_3 \tanh(G_3)] c_2 e^{i(k_2 x - \omega_2 t)}\},
\end{aligned} \tag{5}
$$

where M and M_i $(i, m = 1, 2)$ are both 2×2 matrices and their elements are

$$
\begin{aligned}
M_{mj} &= \frac{2[e^{i(X_j - \overline{X}_m)} + \delta_{mj}]}{(\lambda_j + \mu_j) - (\lambda_m + \overline{\mu}_m)}, \\
(M_i)_{mj} &= M_{mj} - 2\beta_{j,i} e^{i(X_j - \overline{X}_m)},
\end{aligned}
$$

$$
\begin{aligned}
X_j &= \mu_j x + (\lambda_j \mu_j + \frac{1}{2}\mu_j^2 - \frac{1}{2}\lambda_j^2)t, \\
\beta_{j,i} &= \frac{1}{\lambda_j + \mu_j + k_i}, \\
\delta_{mj} &= \begin{cases} 0, & m \neq j \\ e^{2\alpha_m \mu_{I,m}}, & m = j \end{cases}.
\end{aligned}
$$

There is a DW and a bubble or a droplet in each component, the interactions of them can be observed analytically and exactly. All these solutions for describing collision between DWs are absent in Refs. [17] and [18], which were investigated numerically. As an example, we show one case in Fig. 6, for which DW collides with bubble or droplet in two components. It is seen that the profile of kink state does not vary after collision process, but the bubble and droplet state both vary after the collision. Namely, the bubble state in q_1 component transit to be a droplet state after collision (see the upper picture in Fig. 6), and the process is inverse in the q_2 component (see the lower picture in Fig. 6). The collision with a kink makes the bubble-droplet state change greatly. The collision process also induce particle transition between the two components, and this transition behavior can be calculated directly by the particle number in the bubble state.

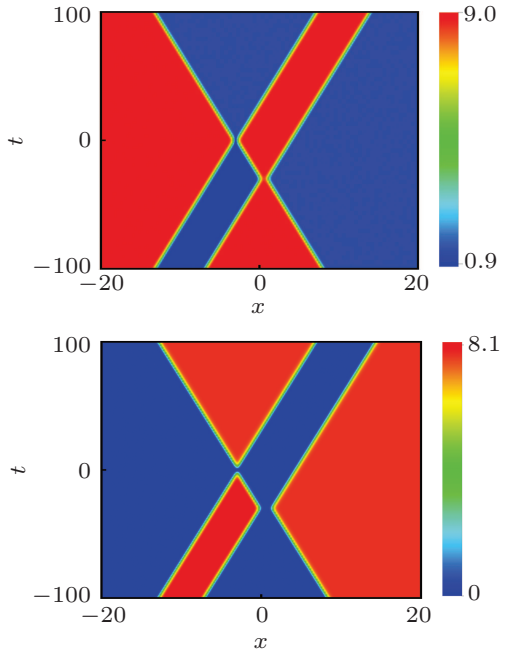


Fig. 6. Density map of collision between domain wall and a bubble-droplet state. It is seen that the bubble-droplet transit to be a droplet-bubble state after colliding with the domain wall, and the domain wall keeps unchanged. This suggests that particle transition happens greatly and fast during the colliding process. The parameters are $\lambda_1 = \lambda_3 = 0.4$, $\lambda_2 = 0.6$, $k_1 = k_2 = 1$, $c_1 = c_2 = 3$, $-\alpha_1 = \alpha_2 = \alpha_3 = 3$.

Finally, we would like to investigate the collision between two bubble-droplets. The general solution for observing their interaction can be given as

$$q_1 = \frac{1}{2}\{c_1 \frac{|M_1|}{|M|} e^{i(k_1 x - \omega_1 t)} + c_2 \frac{|M_2|}{|M|} e^{i(k_2 x - \omega_2 t)}\},$$

$$q_2 = \frac{1}{2}\{c_1 \frac{|M_1|}{|M|} e^{i(k_1 x - \omega_1 t)} - c_2 \frac{|M_2|}{|M|} e^{i(k_2 x - \omega_2 t)}\}.$$

We investigate the collision between bubble-droplets based on the solution analytically. As an example, we show one case in Fig. 7. The two bubble-droplet states are both kept well after the collision process, but there is a striking transition behavior during the collision process. Two droplet states collide with each other, and there is a state with no particles in the q_2 component (see the lower picture in Fig. 7). The particles all transit to q_1 component, therefore there is a hump emerging during the collision between two bubbles (see the upper picture in Fig. 7). In fact, the collision process can be also related with the ones in Fig. 6, since a bubble-droplet is constituted of one DW and one anti-DW. Namely, this situation can also be seen as a bubble-droplet colliding successively with a DW and an anti-DW, there are two collisions with DW in this way. The first collision with a DW changes the bubble-droplet to be droplet-bubble state, and the second collision with an anti-DW changes it back to be a bubble-droplet state. Therefore collision with DWs always induce the transition effect in the BEC with pair-particle transition effects discussed here.

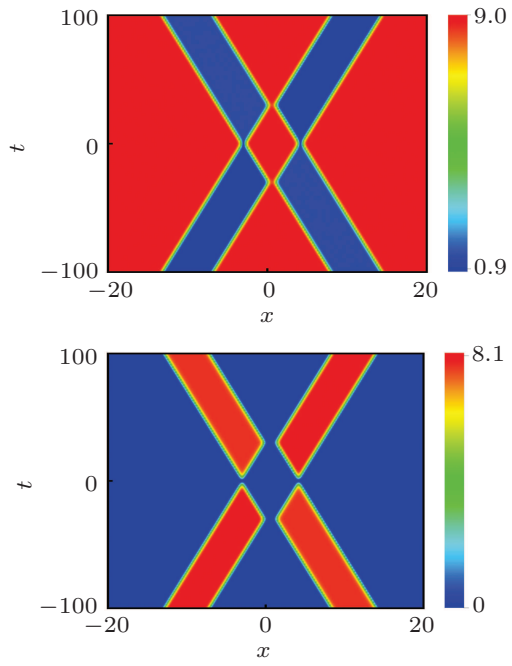


Fig. 7. Density map of collision between two bubble-droplets. It is seen that the collision can be elastic for two bubble-droplets, but many particles in q_2 component transit to q_1 component and transit back perfectly during the collision process. The parameters are $\lambda_1 = \lambda_3 = 0.4$, $\lambda_2 = \lambda_4 = 0.6$, $k_1 = k_2 = 1$, $c_1 = c_2 = 3$, $\alpha_1 = \alpha_4 = -3$, $\alpha_2 = \alpha_3 = 3$.

If we change the relative velocity between two bubbles (droplets), there will be some different transition behaviors at the center of collision, which reminds us that relative velocity will influence the particle transition. As an example in Fig. 8. It is seen that the particle transition is quite different from the one in Fig. 7. The particle transition directions are inverse with each other for the ones in Fig. 7 and Fig. 8. This comes from the phase shifts induced by DW collisions are different for the two cases. It should be noted that the velocity of DW should be smaller than the velocity of sound on the density background with repulsive interactions between atoms.

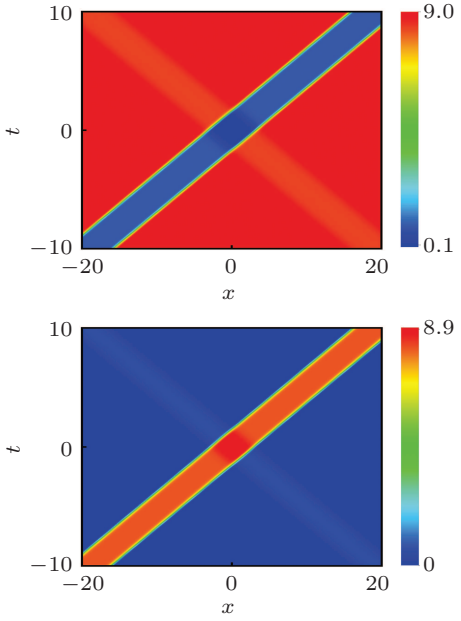


Fig. 8. A bubble(droplet) collides with a bubble(droplet) at a large relative velocity. The transition behavior during collision is different from the low speed case in Fig. 7. The parameters are $\lambda_1 = \lambda_3 = -1.4$, $\lambda_2 = \lambda_4 = 2.4$, $k_1 = k_2 = 1$, $c_1 = c_2 = 3$, and $\alpha_1 = \alpha_4 = -3$, $\alpha_2 = \alpha_3 = 3$.

5. Conclusion and discussion

In this paper, we give the analytical DW solution in two-component BEC which can be described by coupled NLSEs with pair-transition effects. It is shown that DWs can be described exactly by kink and anti-kink excitations in each component. Bubble-droplet structures can be also obtained from the fundamental DW, and their interactions are investigated analytically. Especially, DW interactions demonstrate some striking particle transition dynamics. In contrast to the collision between solitons or other nonlinear waves, these striking transition effects makes the DW admit quite different collision behavior. The collision between kinks induces some phase shift, which makes the DW profile change greatly. Their collisions can be elastic or inelastic with proper combination of fundamental DWs. For examples, collisions between bubble-droplet states can be elastic, and the collision with one DW is usually inelastic. These characters can be used to manipulate one domain wall or bubble-droplet state by interacting with other DWs.

References

[1] Kevrekidis P G, Frantzeskakis D J and Carretero-Gonzalez R 2008 *Emergent Nonlinear Phenomena in Bose–Einstein Condensates: Theory and Experiment* (Berlin: Springer-Verlag)
[2] Berano T M, Gokroo V, Khamehchi M A, Abroise J D, Frantzeskakis D J, Engles P and Kevrekidis P G 2018 *Phys. Rev. Lett.* **120** 063202
[3] Zhang X F, Hu X H, Liu X X and Liu W M 2009 *Phys. Rev. A* **79** 033630
[4] Nistazakis H E, Frantzeskakis D J, Kevrekidis P G, Malomed B A and Carretero-González R 2008 *Phys. Rev. A* **77** 033612
[5] Bo X and Gong J 2010 *Phys. Rev. A* **81** 033618
[6] Alotaibi M O D and Carr L D 2017 *Phys. Rev. A* **96** 013601
[7] Becker C, Stellmer S, Panahi P S, Dorscher S, Baumert M, Richter E M, Kronjager J, Bongs K and Sengstock K 2008 *Nat. Phys.* **4** 496
[8] Hoefer M A, Chang J J, Hamner C and Engels P 2011 *Phys. Rev. A* **84** 041605
[9] Qu C, Pitaevskii L P and Stringari S 2016 *Phys. Rev. Lett.* **116** 160402
[10] Qu C, Tylutki M, Stringari S and Pitaevskii L P 2017 *Phys. Rev. A* **95** 033614
[11] Danaila I, Khamehchi M A, Gokhroo V, Engels P and Kevrekidis P G 2016 *Phys. Rev. A* **94** 053617
[12] Gallemí A, Pitaevskii L P, Stringari S and Recati A 2018 *Phys. Rev. A* **97** 063615
[13] Malomed B A, Nistazakis H E, Frantzeskakis D J and Kevrekidis P G 2004 *Phys. Rev. A* **70** 043616
[14] Kasamatsu K and Tsubota M 2004 *Phys. Rev. Lett.* **93** 100402
[15] Kevrekidis P G, Susanto H, Carretero-Gonzalez R, Malomed B A and Frantzeskakis D J 2005 *Phys. Rev. E* **72** 066604
[16] Kuo Y C, Lin W W and Shieh S F 2005 *Physica D* 211
[17] Filatrella G, Malomed B A and Salerno M 2014 *Phys. Rev. A* **90** 043629
[18] Dror N, Malomed B A and Zeng J 2011 *Phys. Rev. E* **84** 046602
[19] Son D T and Stephanov M A 2002 *Phys. Rev. A* **65** 063621
[20] Merhasin M I, Malomed B A and Driben R 2005 *J. Phys. B: At. Mol. Opt.* **8** 877
[21] Niederberger A, Malomed B A and Lewenstein M 2010 *Phys. Rev. A* **82** 043622
[22] Lv X and Tian B 2012 *Phys. Rev. E* **85** 026117
[23] Lv X and Ling L 2015 *Chaos* **25** 123103
[24] Zhao L C, Ling L, Yang Z Y and Liu J 2015 *Commun. Nonlinear Sci. Numer. Simul.* **23** 21
[25] Ling L and Zhao L C 2015 *Phys. Rev. E* **92** 022924
[26] Qin Y H, Zhao L C, Yang Z Y and Yang W L 2018 *Chaos* **28** 013111
[27] Manakov S V 1974 *Sov. Phys. JETP* **38** 248
[28] Fölling S, Trotzky S, Cheinet P, *et al.* 2007 *Nature* **448** 06112
[29] Zöllner S, Meyer H D and Schmelcher P 2008 *Phys. Rev. Lett.* **100** 040401
[30] Bader P and Fischer U R 2009 *Phys. Rev. Lett.* **103** 060402
[31] Fischer U R, Lee K S and Xiong B 2011 *Phys. Rev. A* **84** 011604
[32] Malomed B A 1990 *Phys. Rev. A* **42** 7244
[33] Zhao L C, Ling L, Yang Z Y and Liu J 2016 *Nonlinear Dyn.* **83** 659
[34] Zhao L C, Ling L, Yang Z Y and Yang W L 2017 *Nonlinear Dyn.* **88** 2957